

Theoretical Analysis of SAW Propagation Characteristics in (100) Oriented AlN/Diamond Structure

Chia-Chi Sung, Yuan-Feng Chiang
Department of Engineering Science
and Ocean Engineering
National Taiwan University
Taipei, Taiwan, R. O. C.
d93525005@ntu.edu.tw

Ruyen Ro, *senior member, IEEE*,
Ruyue Lee
Department of Electrical Engineering
I-Shou University
Kaohsiung, Taiwan, R. O. C.
ryro@isu.edu.tw

Sean Wu, *member, IEEE*
Department of Electronics Engineering
and Computer Science
Tung-Fang Institute of Technology
Kaohsiung, Taiwan, R. O. C.
wusean.tw@gmail.com

Abstract—The surface acoustic waves (SAWs) propagating in interdigital transducer (IDT)/(100) aluminum nitride (AlN)/diamond possess the greater phase velocity and coupling coefficient than those in IDT/(002) AlN/diamond. In this study, the finite element method (FEM) is employed to calculate SAW characteristics in these two layered structures with different electric interfaces; i.e., IDT/AlN/diamond, AlN/IDT/diamond, IDT/AlN/thin metal film/diamond, and thin metal film/AlN/IDT/diamond. The effects of Cu and Al electrodes on SAW characteristics are illustrated. Simulation results show that the Cu IDT/(100) AlN/diamond structure can support a SAW with a coupling coefficient of 1.71%, a phase velocity of 9705 m/s, and a reflectivity of 0.15, which is applicable for the miniaturized wideband and super high band applications.

Keywords— surface acoustic wave; AlN; diamond; finite element method; reflectivity

I. INTRODUCTION

Increasing demand for communication devices with miniaturized components has made the surface acoustic wave (SAW) devices widespread used in daily states. There are several methods to enhance the characteristics of SAW devices for super high frequency applications, including usage of high speed piezoelectric materials, leaky SAWs, employment of ultrafine electrode by using high-resolution lithography, or layered structures combined with high speed material. In the case of layered structure, diamond is an attractive non-piezoelectric material because it possesses the highest acoustic wave velocity among all materials. The high frequency SAW devices based on diamond are commonly combined with piezoelectric films such as aluminum nitride (AlN) or zinc oxide (ZnO), which are applicable in the GHz range [1–7].

AlN has a SAW velocity of 5600 m/s, which is higher than 2700 m/s of ZnO. As a result, researchers commonly use AlN films on a diamond substrate to acquire low velocity dispersion. For (100) AlN/(111) diamond structures, the maximum values of coupling coefficient, K^2 , and associated effective phase velocity, v_{eff} , are 2.3% and 10500 m/s, respectively, where the propagation direction is parallel to the c-axis and the a-axis is perpendicular to the diamond surface [5]. SAW device in (100) AlN/(111) diamond structure can

attain a higher phase velocity and a larger coupling coefficient than that in (002) AlN/(111) diamond structure [5].

In addition to a high phase velocity and large K^2 , designing low-loss and miniature SAW devices such as single phase unidirectional transducers (SPUDTs), RF filters and duplexers requires a large reflectivity in the interdigital transducers (IDTs) [8–15]. For example, Kadota *et al.* suggested a reflection coefficient of 0.15 for designing wideband code division multiple access (WCDMA) duplexers [11]. Generally, reflectivity depends upon the geometry and material constants of the electrode, e.g. its thickness, width, Young's modulus, Poisson's ratio, and mass density. To noticeably reduce the device size with the designed gratings, researches have studied the usage of high density metal electrode such as W, Pt, Ta, Au, Ta, and Cu in layered structures [14]. For example, Cu IDTs provide larger mechanical reflection and smaller electric resistance than Al IDTs. Moreover, the sideband suppression capability and insertion loss of the filters employing the SPUDTs can be improved by using high density metal electrode [12].

The purpose of this study is to determine the SAW characteristics of a diamond layered structure combined with either (002) or (100) oriented AlN films by taking the mass effects of electrode into consideration. The finite element method (FEM) is employed to calculate SAW characteristics in four layered structures, including IDT/AlN/diamond, AlN/IDT/diamond, IDT/AlN/thin metal film/diamond, and thin metal film/AlN/IDT/diamond. The effects of Cu and Al electrodes are illustrated.

II. METHODOLOGY

Figure 1 illustrates the layered structures with various IDT and/or thin metal film positions, where h_F and h_E denote the thicknesses of the AlN films and electrode, respectively, p represents the electrode pitch, and λ is the wavelength. The IDT/AlN/diamond, IDT/AlN/thin metal film/diamond, AlN/IDT/diamond, and thin metal film/AlN/IDT/diamond structures will be denoted hereafter as SFT, SMFT, STF, and STFM, respectively, where S stands for the diamond substrate, F the AlN film, T the IDT, and M the thin metal film [16].

The FEM is employed to calculate the propagation the

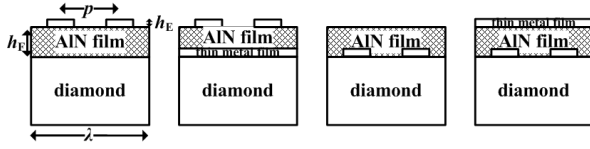


Figure 1. Schematic of four layered structures.

characteristics of SAWs in those four structures, including coupling coefficient, effective phase velocity, and reflectivity [9, 17]. By the use of the FEM, the eigenfrequency pairs of asymmetric and symmetric modes can be obtained by inspecting the mechanical and electric displacement fields for two different IDT boundary conditions, shorted and open IDTs. The effective phase velocity is given by

$$v_{\text{eff}} = p(f_{\text{asym}} + f_{\text{sym}}), \quad (1)$$

where f_{asym} and f_{sym} are the eigenfrequencies of asymmetric and symmetric modes, respectively. The coupling coefficient can be determined from

$$K^2 = 2(v_f - v_m) / v_f, \quad (2)$$

where v_f and v_m are calculated using (1) with open and shorted IDTs, respectively. The reflectivity per electrode can also be obtained from the corresponding eigenfrequencies as given by

$$kp = \pi(f_{\text{asym}} - f_{\text{sym}}) / (f_{\text{asym}} + f_{\text{sym}}). \quad (3)$$

III. RESULTS AND DISCUSSIONS

It was reported that the second mode of SAWs exhibits the largest K^2 among first five modes in either (100) or (002) AIN films on diamond [5]. Therefore, the second mode is chosen in the following investigations. The material constants used in this study were obtained from Benetti *et al.* [3] and Gualtieri *et al.* [18]. The optimum thickness of the AIN film is determined first from the coupling coefficient curves without considering the mass effect of the IDTs. In (002) AIN/diamond structures, the maximum K^2 in the SFT, SMFT, STF, and STFM structures are 1.316%, 2.31%, 1.47%, and 3.09%, at the corresponding (002) AIN films thickness-to-wavelength ratios, h_f/λ , of 0.5, 0.23, 0.24, and 0.22, respectively. In (100) AIN/diamond structures, the maximum K^2 in the SFT, SMFT, STF, and STFM structures are 2.381%, 1.9%, 2.92%, and 1.73%, at h_f/λ being equal to 0.3, 0.38, 0.214, and 0.23, respectively. These optimum AIN thicknesses are applied in the following discussion.

Taking the effects of IDTs into account, Figs. 2 and 3 show the calculated effective phase velocity curves in the four structures with different oriented AIN films. A reduction in the effective phase velocity is observed with the increase of the electrode thickness. For each structure, the decreasing rate of Cu electrode is larger than that of Al electrode and, hence, the phase velocity using Al electrode is greater than that of Cu electrode.

Figures 4 and 5 present the corresponding K^2 . The coupling coefficient in both figures exhibits a decreasing tendency as h_f/λ increases. In Fig. 4, a maximum K^2 3.1% is observed in

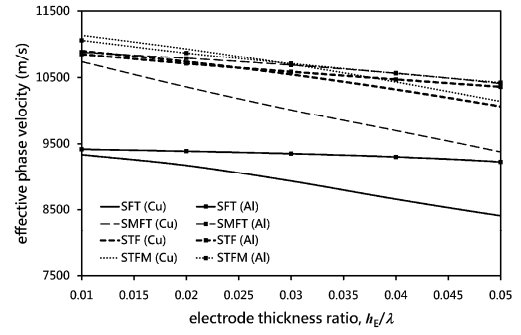


Figure 2. Calculated effective phase velocity dispersion curves in the four structures with (002) AIN film and different electrode materials versus electrode thickness-to-wavelength ratio, h_f/λ .

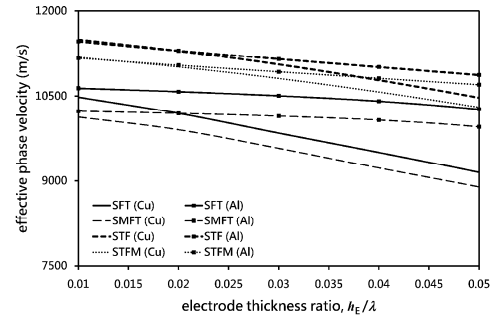


Figure 3. Calculated effective phase velocity dispersion curves in the four structures with (100) AIN film and different electrode materials versus electrode thickness-to-wavelength ratio, h_f/λ .

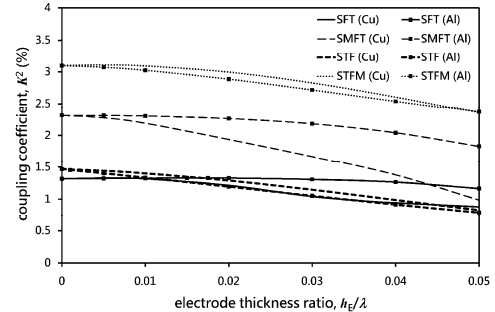


Figure 4. Calculated electromechanical coupling coefficient in the four structures with (002) AIN film and different electrode materials versus electrode thickness-to-wavelength ratio, h_f/λ .

the STFM (Cu) curve at h_f/λ 0.5%. The STF (Al) curve possesses the best K^2 of 3.17% in Fig. 5 at h_f/λ 3%.

Figures 6 and 7 show the reflectivity per electrode for all four structures with (100) and (002) oriented AIN films versus h_f/λ . As mentioned in the Introduction Section, a reflection coefficient of 0.15 was suggested by Kadota *et al.* for the design of WCDMA duplexers [11]. The SFT structure with Cu electrode, as presented in Figs. 2, 4, and 6, shows a reflectivity of 0.15 at h_f/λ 3.8% with an associated effective phase velocity of 8717 m/s and K^2 0.95%. Referred to Figs. 3, 5, and 7, the

SFT and SMFT structures with Cu electrode have the reflectivity of 0.15 at h_E/λ 3.4% and 3.2%, respectively, with an associated effective phase velocity of 9705 m/s and 9504 m/s, and the K^2 of 1.71% and 1.6%. This implies that the Cu IDT/(100) AlN/diamond structure is a promising candidate for the wideband and super high band applications.

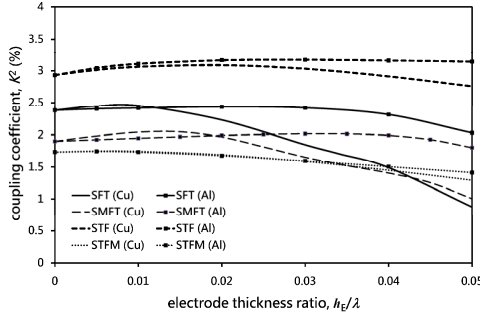


Figure 5. Calculated electromechanical coupling coefficient in the four structures with (100) AlN film and different electrode materials versus electrode thickness-to-wavelength ratio, h_E/λ .

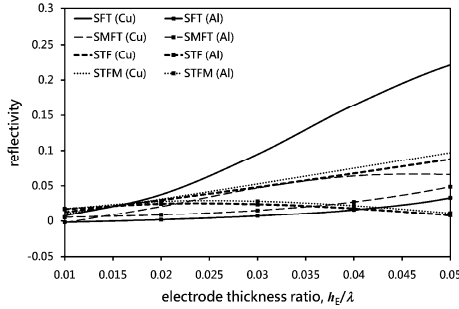


Figure 6. Calculated reflectivity in the four structures with (002) AlN film and different electrode materials versus electrode thickness-to-wavelength ratio, h_E/λ .

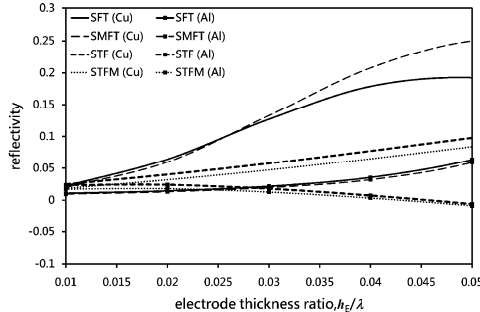


Figure 7. Calculated reflectivity in the four structures with (100) AlN film and different electrode materials versus electrode thickness-to-wavelength ratio, h_E/λ .

IV. CONCLUSIONS

This study investigates the phase velocities, electromechanical coupling coefficients, and reflectivities of the second mode of SAW in IDT/AlN/diamond,

AlN/IDT/diamond, IDT/AlN/thin metal film/diamond, and thin metal film/AlN/IDT/diamond structures. A reflectivity larger than 0.25 can be obtained by using the Cu electrode in AlN/diamond layered structures. The coupling coefficient and phase velocity decrease as the electrode thickness increases. Simulation results show that the Cu IDT/(100) AlN/diamond structure can supports a SAW with a coupling coefficient of 1.71% and a phase velocity of 9705 m/s at $h_E/\lambda=0.3$ and $h_E/\lambda=3.4\%$, and with a reflectivity of 0.15. This information will be beneficial in designing the SAW device for super high frequency band and wideband applications by using AlN/diamond layered structures.

ACKNOWLEDGMENT

The authors would like to thank the National Science Council of the Republic of China for financially supporting of this research under Contract NSC 96-2221-E-002-299-MY3 and NSC 97-2221-E-214-023, and special thanks to the Ministry of Education of the Republic of China for the conference support.

REFERENCES

- [1] F. Benedic, M. B. Assouar, P. Kirsh, D. Moneger, O. Brinza, O. Elmazria, P. Alnot, and A. Gicquel, "Very high frequency SAW devices based on nanocrystalline diamond and aluminum nitride layered structure achieved using e-beam lithography," *Diamond and Related Materials*, vol. 17, pp. 804–808, October 2007.
- [2] G. F. Iriarte, "Surface acoustic wave propagation characteristics of aluminum nitride thin films grown on polycrystalline diamond," *Journal of Applied Physics*, vol. 93, pp. 9604–9609, June 2003.
- [3] M. Benetti, D. Cannat'a, F. D. Pietrantonio, and E. Verona, "Growth of AlN piezoelectric film on diamond for high-frequency surface acoustic wave devices," *IEEE Transactions on Ultrasonics, Ferroelectrics, and Frequency Control*, vol. 52, pp. 1806–1811, October 2005.
- [4] P. Kirsch, M. B. Assouar, O. Elmazria, V. Mortet, and P. Alnot, "5 GHz surface acoustic wave devices based on aluminum nitride/diamond layered structure realized using electron beam lithography," *Applied Physics Letters*, vol. 88, pp. 223504–223505, May 2006.
- [5] S. Wu, R. Ro, Z. X. Lin, and M. S. Lee, "Rayleigh surface acoustic wave modes of IDT/(100) AlN/(111) diamond," *Journal of Applied Physics*, vol. 104, pp. 064919-1–064919-4, September 2008.
- [6] S. Wu, R. Ro, and Z. X. Lin, "Rayleigh surface acoustic wave modes of (100) ZnO films on (111) diamond," *Applied Physics Letters*, vol. 94, pp. 032908-1–032908-3, January 2009.
- [7] S. Wu, R. Ro, Z. X. Lin, and M. S. Lee, "High velocity shear horizontal surface acoustic wave modes of interdigital transducer/(100) AlN/(111) diamond," *Applied Physics Letters*, vol. 94, pp. 092903-1–092903-2, March 2009.
- [8] D. P. Morgan, *Surface Acoustic Wave Filters*, 2nd ed., Academic Press, 2007.
- [9] K. Y. Hashimoto, *Surface Acoustic Wave Devices in Telecommunications: Modeling and Simulation*, 1st ed., Springer, 2000, pp. 214–218.
- [10] C. C. Ruppel and T. A. Fjeldly, *Advances in Surface Acoustic Wave Technology, Systems and Applications*, 1st ed., vol. 2. World Scientific Publishing Company, 2001, pp. 39–47.
- [11] M. Kadota, T. Nakao, K. Nishiyama, S. Kido, M. Kato, R. Omote, H. Yonekura, N. Takada, and R. Kita, "Small surface acoustic wave duplexer for wide-band code-division multiple access," *Japanese Journal of Applied Physics*, vol. 46, pp. 4714–4717, July 2007.
- [12] H. Li, J. Wen, K. Y. Hashimoto, T. Omori, and M. Yamaguchi, "Low-loss and constant-group-delay surface acoustic wave filters employing Cu-based resonant single-phase unidirectional transducers," *Japanese Journal of Applied Physics*, vol. 45, pp. 4655–4657, May 2006.

- [13] T. Omori, S. Nakagomi, H. Tanaka, H. Asano, K. Y. Hashimoto, and M. Yamaguchi, "SAW reflection characteristics of Cu electrodes and their application to SAW IF devices," *Proceedings of the IEEE Ultrasonics Symposium*, pp. 19–23, October 2002.
- [14] M. Kadota, T. Nakao, N. Taniguchi, E. Takata, M. Mimura, K. Nishiyama, T. Hada, and T. Komura, "SAW substrate for duplexer with excellent temperature characteristics and large reflection coefficient realized by using flattened SiO₂ film and thick heavy metal film," *Proceedings of the IEEE MTT-S International Microwave Symposium*, pp. 382–385, June 2006.
- [15] M. Kadota, "High performance and miniature surface acoustic wave devices with excellent temperature stability using high density metal electrodes," *Proceedings of the IEEE Ultrasonics Symposium*, pp. 496–506, October 2007.
- [16] C. Caliendo, "Analysis of dispersive electroacoustic coupling structures for application to gigahertz-band, temperature-compensated AlN-based acoustic devices," *Applied Physics Letters*, vol. 92, pp. 103501-1–103501-3, March 2008.
- [17] V. Plessky, J. Koskela, "Coupling-of-modes analysis of SAW devices," *International Journal of High Speed Electronics and Systems*, vol. 10, pp. 867–947, 2000.
- [18] J. G. Gualtieri, J. A. Kosinski, and A. Ballato, "Piezoelectric materials for acoustic wave applications," *IEEE Transactions on Ultrasonics, Ferroelectrics, and Frequency Control*, vol. 41, pp. 53–59, January 1994.